scientific reports

Check for updates

OPEN

Impairment of theta oscillations in the hippocampal CA1 region may mediate age-dependent movement alternations in the 5xFAD mouse model of Alzheimer's disease

Hong Ni[1,4,7], Zhongzhao Guo[1,5,6,7], Jie Wang[3,7], Zilu Zhu[1], Chenyi Xia[1], Ming Xu[1], Guohui Zhang[4✉] & Deheng Wang[1,2✉]

Clinical evidences indicate that multifaceted gait abnormalities may manifest in Alzheimer's disease (AD) patients, which are associated with cognitive decline. Although the correlation between hippocampal theta power and locomotion has been known for a long time, the mechanisms by how hippocampal impairment participates in the altered gait seen in AD is not fully understood. To explore the manifestations of gait disorders in AD, we characterized gait performance in 3-, 6-, and 9-month-old male 5xFAD and control mice in the semi-automated, highly sensitive, Catwalk XT system. The 5xFAD mice displayed a decrease in kinetic parameters (average speed and cadence), and spatial parameters (paw area), while the temporal parameters (stance and swing time) were significantly increased. The parameters of interlimb coordination also displayed deficits. The majority of impairment variables related to the slow speed in 5xFAD mice at 9-month-old. We further explored the theta oscillations in the brain by in vivo tetrode recording of the hippocampal CA1. The results showed that the theta oscillations reduced in the hippocampal CA1 of 5xFAD mice, which related to the gait impairments. In conclusion, gait impairments started at 6 months of age, manifested at 9 months of age in 5xFAD mice. A reduction in theta oscillation power of the hippocampal CA1 may be responsible for the gait impairments.

Keywords Alzheimer's disease, 5xFAD mouse, Gait, Hippocampus, Theta oscillations

Alzheimer's and other neurological disorders of the central nervous system (CNS), such as Stroke, Parkinson's, and Huntington's diseases, adversely affect communication and motor functions. A prominent characteristic of these disorders is the manifestation of abnormal gait patterns. Gait is an intricate and learned biological activity initiated by voluntary motion[1]. It involves one leg bearing the body's weight (BW) while the other advances to initiate the next move, necessitating a repetitive, smooth, and naturally synchronized balance with each step[2]. This process produces distinct gait patterns that can be used to evaluate personnel health, specifically in older adults[3]. Gait is a multifaceted activity that necessitates the coordination of limb movement, postural control, balance, movement adjustment, and cadence. Speed regulation is an important aspect of locomotion. Changes in locomotor speed may also result in coordination between limbs, which can contribute to specific patterns of limb movement or gaits due to the synchronized pattern of muscle activity. Quadrupeds show various speed-dependent locomotor gaits[4].

[1]School of Integrative Medicine, Shanghai University of Traditional Chinese Medicine, Shanghai 201203, China. [2]Engineering Research Center of Traditional Chinese Medicine Intelligent Rehabilitation, Shanghai University of Traditional Chinese Medicine, Shanghai 201203, China. [3]Department of Chinese Medicine & Integrative Medicine, Shanghai Geriatric Medical Center, Zhongshan Hospital, Fudan University, 2560 Chunshen Road, Shanghai 201104, China. [4]Rehabilitation department, Yueyang Hospital of Integrated Traditional Chinese and Western Medicine, Shanghai 200437, China. [5]Department of Rehabilitation Medicine, Tong Ren Hospital, Shanghai Jiao Tong University School of Medicine, Shanghai 200336, China. [6]Institute of Rehabilitation, Shanghai Jiao Tong University School of Medicine, Shanghai 200025, China. [7]Hong Ni, Zhongzhao Guo, Jie Wang contributed equally to this work. ✉email: yyyyzgh827@126.com; wangdeheng@shutcm.edu.cn

Alzheimer's disease (AD) is a neurodegenerative age-related disease that is marked by the presence of neurofibrillary tangles, Aβ plaques, and cognitive impairment[5]. Some studies have found a significant association between a decrease in gait function and AD, besides the cognitive impairment that is the main characteristic of AD[6–8]. Impairments in gaits have been identified as biomarkers for the early stages of the disease, which can be used to predict cognitive impairment in older adults[9–11]. It has been observed that patients with mild cognitive impairment (MCI) who also experience motor dysfunction are more likely to develop AD than those with MCI alone. The severity of cognitive malfunction in patients with AD is frequently associated with motor dysfunction[12]. Compared to normal aging[13], AD was associated with gait characteristics and defined by a slower pace, impaired rhythm, and increased variability. Gait variability can be described using various parameters. For example, stride time variability indicates the ability to generate consistent rhythmical stride cycles, whereas step width and double limb support indicate postural control mechanisms during gait[14]. Currently, there is no established protocol to evaluate gait variability, as evidenced by the inconsistency in data acquisition techniques, distance walking, instrumentation, and analytical algorithms[15]. However, high gait variability was regarded as a sign of cognitive-cortical dysfunction, which may facilitate the diagnosis of AD[16]. This study also illustrated that patients with AD usually walk at a slowed pace, and their condition worsens as it progresses[17]. Moreover, gait disturbances are a significant concern due to reduced mobility, which has a detrimental effect on the quality of life, and increased falls can elevate the risk of morbidity and mortality[18]. It may be beneficial to perform continuous and consistent monitoring of the mobility performance of older adults to diagnose and evaluate the extent of neurological impairment[19].

Due to conserved similarities between rodent and human locomotion, motor deficits are often studied qualitatively in rodent models using the beam balance rod, inverted screen, grip strength, and rotarod tests[20], as this quantifies the efficacy of different therapeutic approaches. However, a significant drawback of these motor tests is that they rely on the expertise of a trained observer who can only identify major motor and coordination dysfunctions[21]. Recent application of automated systems and technology has enabled the quantitative evaluation of motor deficits, independent of the observer's existence, *via* CatWalk gait analysis.

Despite the differences in gait patterns between rodents and humans, the basic rules for analyzing these patterns remain the same[22,23]. Thus, advanced analysis of rodent gait can be essential for better modeling human disorders. Considering the increasing importance of the association between AD and human gait, several studies are now focused on characterizing the gait change in AD mouse models. For example, Brown et al. discovered a decrease in locomotion activity in 11 to 13-month-old 5xFAD mice, potentially due to problems with their gait[24,25]. Similarly, in the Tg2576 mouse model of AD, Seo et al. reported significant reductions in stride times and increases in cadence before plaque accumulation, irrespective of body size or weight[26]. Gait abnormalities were also present in the 6-month-old 3xTg-AD mice, whose strides were shorter than wild-type (WT) mice[27]. However, the effects of AD on various gait parameters of 5xFAD mouse models of different ages are yet to be well characterized. Therefore, this study compared gait function in freely moving 3-, 6- and 9-month-old male 5xFAD mice and age-matched WT controls using the Catwalk XT system to analyze gait parameters (e.g., stride time and length, cadence, swing speed, and average speed). Based on previous studies that demonstrated gait abnormalities in AD mice, these parameters are considered sensitive indications of aberrant human mobility associated with AD[16].

Moreover, the corresponding brain characteristics have been extensively investigated, as variations in locomotion can predict slight alterations that occur due to impaired cognition or aging. It is widely recognized that the hippocampus is crucial for cognition, navigation, and memory[28]. Significantly, the medial entorhinal cortex and the CA1 region of the hippocampus have been associated with linear speed modulation, either with positional information or speed cells[29,30]. Theta power was also related to locomotor activity measured at the hippocampal field potential, where speed was influenced[31,32]. The amplitude and frequency of theta rhythms increased in hippocampal CA1 as walking speed increased[33], indicating a possible role in coding speed. Gait speed is specifically encoded by variations in the firing rates of neurons in the entorhinal cortex and the hippocampus[29,34–36]. Several entorhinal neurons demonstrate changes in firing rhythmicity with increased walking speed, most commonly growing their frequency[37]. Previously, preclinical and clinical models of AD have reported reduced theta power in the CA1 region of the hippocampus[38–40]. Previous studies have extensively discovered the association between the hippocampus and movement[41,42]. However, the mechanisms by which hippocamp impairment contributes to the altered locomotion observed in AD remain unclear. Therefore, the role of the CA1 region of the hippocampus in modulating gait speed was further investigated using tetrode in vivo recording during walking in an open field test (OFT) to determine whether it contributed to a gait deficit in 5xFAD mice.

This study reported that 5xFAD mice show significant impairment in gait behavior, particularly at 9 months of age, possibly due to functional abnormalities such as reduced theta oscillations power and decreased speed-correlated cell proportions within the hippocampal CA1.

Methods

Animal grouping

5xFAD mice and age-matched C57BL/6 (J strain) WT mice were obtained from the Model Animal Research Center of Nanjing University and bred in the Experimental Animal Center of Shanghai University of Traditional Chinese Medicine. 3-, 6- and 9-m old mice ($n = 10$ in each group) were used in studies. All mice (5 per cage) were housed in an environment with a temperature of $22 \pm 2°$ C and humidity of $55 \pm 10\%$ under a 12-h light/dark cycle (light on 07:00–19:00) and had access to water and food ad libitum. Before experiment all mice were allowed to have seven days acclimation. All experimental protocols were in strict accordance with the regulations of the National Institutes of Health guide for the care and use of laboratory animals, formulated by the Ministry

of Science and Technology of the People's Republic of China and were approved by the Animals Research Ethics Committee of Shanghai University of Chinese Medicine (No.PZSHUTCM200821019).

Genotyping

5×FAD mice are APP/presenilin 1 (PS1) double transgenic mice that express 5 familial forms of AD (5×FAD) mutations, which express the 695-amino acid isoform of the human APP (APP695) carrying the Swedish (K670N/M671L), Florida (I716V), and London (V717I) mutations and human PSEN1 carrying the M146L/L286V mutations, and Heterozygous mice were maintained by crossing with C57BL/6 mice. Both were obtained from Model Animal Research Center of Nanjing University (Nanjing, China). Genotyping was performed as previously described[43].The tails of mice (21 days after birth) were cut off with a length of 3–5 mm and placed into the corresponding EP tube for genetic identification. Total DNA was isolated from the mice tails by DNA extraction kit (Beijing Tiangen Biochemical Technology, China) for PCR experiment. 10 μL2 × Taq mix, 1 μL primer, 1μLDNA, and ddH2O supplement to 20 μL were added into each PCR tube for PCR amplification. For APP/PS1 the following protocol was used: initial denaturation for 5 min at 95℃, followed by 35 cycles of (denaturation for 30 sec at 95℃, annealing for 30 sec at 66℃, and extension for 30 sec at 72℃), followed by a final extension for 10 min at 72℃, 4℃ store. Primers (Sangon Biotech, China) used for PCR of 5×FAD mice are set as following. PS1 forward: 5'-AATAGAGAACGGCAGGAGCA-3', PS1 reverse: 5'-GCCATGAGGGCACTAATCAT-3'. WT forward: 5'-CTAGGCCACAGAATTGAAAGATCT-3', WT reverse: 5'-GTAGGTGGAAATTCTAGCATCATCC-3'. The PCR products were run on 1% agarose gels made with TAE bugger for 30 min (140 V constant voltage) and EB exposed in the exposure instrument (Bio-Rad, USA) to observe the gene bands. With the PCR result (Figure below) we will recognize C57BL/6 (WT) mice and 5×FAD (AD) mice. In the field of Alzheimer's disease research, the 5xFAD model is among the most well-studied and commonly employed mouse models. There are thymus antigen-1 (Thy-1) promoter–driven transgenes for mutated presenilin-1 (PS1) and amyloid precursor protein (APP)[44]. These mice are well adapted for the research of movement impairment in Alzheimer's disease due to the fast onset of AD-related pathology and cognitive failure they exhibit. In addition, consistent with the findings of others, at 6 months of age, these mice start to show motor dysfunction which progresses rapidly to profound motor dysfunction by 9 months[45].

CatWalk gait analysis

To detect the gait differences between 5xFAD and WT mice at different ages, we tested 3-, 6- and 9-m male mice (10 each group), and 9-m female mice (10 each group) using a highly sensitive, automated computer-assisted method (Noldus Information Technology Inc, USA) as described[46]. Catwalk is a sophisticated apparatus that is capable of assessing footfall and motor performance quantitatively, as the animals freely walked on an illuminated glass platform (20 cm wide × 130 cm long), a high-speed high-resolution camera was used to record paw location and placement patterns, providing accurate and repeatable measurements of gait function as well as spatial and temporal aspects of interlimb coordination. We began by establishing the walkway area in accordance with the recommendation of the company. We did not include any light stimuli, food enticements or even the home cage at the end of the walkway as bait in our method in order to achieve unforced locomotion. The mice were placed in the testing room 30 min before the experiments to become accustomed to the conditions of the experiment. Every mouse had a 25-minute free walk along the corridor and walkway on training days. Every trial was followed by the cleaning of the glass plate. A minimum of three completed trials were collected during the testing days, during which the mice were allowed to freely move back and forth on the corridor for 20 min. For mice that were not able to complete the trial in 20 min, a second try was permitted the following day so that at least three compliant trials could be completed without stressing the mice. The high-speed camera was recorded at 100 frames per second (GP-2360 C, GEViCAM) with lenses set at 1.5 apertures (DFGHA–1B Fujifilm). Trials that met compliance criteria were defined as those ranging in duration between 1 and 5 s (where the average speed should be between 8 and 40 cm/s), along with maximum speed variations of not more than 20%. Based on the manual and previous experience[47], the training and experimental protocols were conducted.

The phase coupling parameter describes the temporal relationship between placement of two paws (anchor and target) within a step cycle. It can also be used to examine inter-paw coordination across six pairs of paws (diagonal pairs: RF-LH, LF-RH, ipsilateral pairs: RF-RH, LF-LH, and girdle pairs: LF-RF, LH-RH). A healthy young mouse with normal gait usually moves the diagonal paw pairs synchronously with the anchor, resulting in a 0% phase coupling values. A phase coupling of 50% is expected when ipsilateral and girdle pairs alternate. The phase coupling is expressed as a percentage of the step cycle time of the anchor paw by measuring the timing between initial contacts of paw pairs. In order to determine whether asynchronous stepping occurs, the absolute deviation from the expected coupling value should be calculated. Deviation from the expected value which represents a high level of gait coordination is shown as Δ Phase coupling[48,49].

Subsequently, for the analysis, each foot print was manually checked and labelled as LF (Left Front), LH (Left Hind), RF (Right Front), and RH (Right Hind) paw to generate gait parameters. We categorized the gait parameters into four major categories to better present the data: (1) gait characteristics and kinetic parameters (average speed, cadence, number of steps, body speed and swing speed), (2) temporal parameters (stance and swing time, step cycle and maximum contact at [% of stance time]), (3) spatial parameters (print area and maximum intensity), (4) interlimb coordination parameters (base of support, print position stride length, support, phase coupling, number of patterns, regularity index and step sequences).

Grip strength test

The grip strength meter (Bioseb, Pinellas Park, FL, USA) was used to assess muscle function. In order to help each mouse grasp the grip, its tail was gently pulled on the grip plate. Once the mouse had grasped the grip plate firmly, the tail was pulled until it released its grip. The grip strengths of the forelimb, hindlimb, and the whole

limb were measured. A maximum gripping power was recorded. We repeated the experiment process in three separate trials per animal, and the maximum value across the trials was considered the evaluation value.

Open field test (OFT)

Implanted mice were allowed to freely move in the square arena ($50 \times 50 \times 40$ cm) with white walls and floor for 30 min. The speed and total distance travelled of the mice were recorded and analyzed by CinePlex video tracking system (Plexon, USA). The open field arena was fully cleaned with 75% ethanol after each trial.

Tetrode electrode implantation surgery and data collecting

We used the Self-made movable bundles of the 32-channel tetrode electrode[50] to target the hippocampal CA1 (AP -2 mm; ML ± 1.8 mm and -DV 1.1 mm) of the anesthetized mice on the stereotactic frame. The signals were amplified, band-pass filtered (0.5–1000 Hz for local field potentials [LFPs] and 0.6–6 kHz for spikes), and digitized by the Plexon OmniPle Neural Data Acquisition System (Plexon, USA). Neural signals were recorded by using the Plexon OmniPlex Neural Data Acquisition System (Dallas, TX, USA). Signals were digitized at a frequency of 40 kHz for spikes. When the recording is finished, open the data with Offline Sorter to open for offline processing. The processing includes: wave shape alignment, noise filtering, neuron classification, etc. Then we used custom-made Matlab and followed by manual adjustment using the software MClust 4.4 program (A. D. Redish, http://redishlab.neuroscience.umn.edu/MClust/MClust.html). Through the above steps single units were identified from multi-unit recordings. Last, we used Neuroexplorer 5.306 software (Nex Technologies, USA), Neuroexplorer software correlates neuronal signals with behavioral data.

Statistical analysis

Normality was checked by visual inspection of the data and a Shapiro-Wilks test and p value was more than 0.05. Two-way ANOVA (genotype and age as interacting factors), the Tukey's test or Holm-Sidak test were applied for post hoc comparisons. All correlations were assessed using a linear regression to find an r^2 value and the F-test to determine a p value of the linear fit. All data were presented as means ± SEM and analyzed by GraphPad 7.0 software (San Diego, CA). A p value of < 0.05 was considered as statistically significant.

Results

Gait impairment in 5xFAD mice

Here, we found that compared to WT ones, 5xFAD mice exhibited significant functional impairment in gait that intensify with increasing age (Fig. 1A), manifesting by the following four aspects of gait parameters (1) decreased speed (including average speed and swing speed of all paws), stride length and cadence as well as increased number of steps; (2) spending more time (including stance time, swing time, step cycle time and time for all paws to make the maximum contact to the glass plate); (3) decreased print areas and maximum intensity of all paws; (4) increased base of support and phase coupling deviation of all paws, decreased print position, and regularity index as well as significantly altered step cycle and step patterns of all paws. All the gait parameters that we focused on in our study are shown for each paw, namely the left front (LF), left hind (LH), right front (RF), and right hind (RH) paw. For some data, we only presented single forelimb (RF) and hindlimb (RH) as the data of the other two limbs were similar. In detail, the following is described.
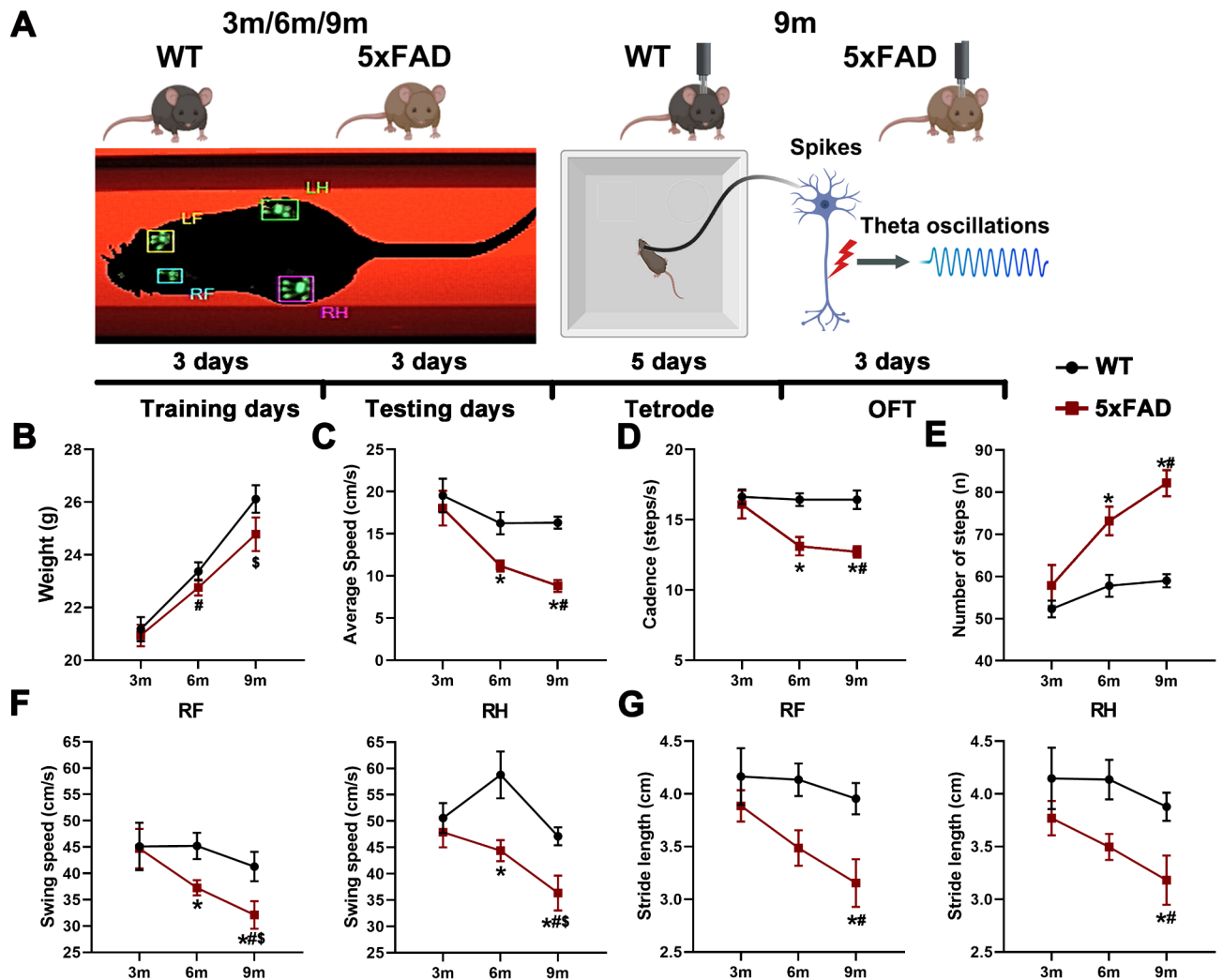
Gait characteristics and kinetic parameters
Firstly, the body weights of mice were examined to determine suitable detection settings. The comparison between 5xFAD mice and WT ones of the same age (3-, 6- and 9-m) revealed no difference, while both of them showed significantly increased body weights with aging (Fig. 1B). The results of gait characteristics and kinetic parameters manifested that from 3- to 9-m old, 5xFAD mice showed a significant decreasing trend in the average speed (F (2, 54) = 11.64, $P < 0.0001$, Fig. 1C) and cadence (F (2, 54) = 4.619, $P = 0.0141$, Fig. 1D) and an increasing tendency in the number of steps with age (F (2, 54) = 12.99, $P < 0.0001$, Fig. 1E) and differences were found in 3- and 9-m old groups. At the same time, we discovered that compared with 6-, and 9-m old WT mice, the age-matched 5×FAD ones showed decreased average speed and cadence and increased number of steps, but there was no difference between 3-m old groups (F (1, 54) = 17.56, $P = 0.0001$, Fig. 1C, F (1, 54) = 23.10, $P < 0.0001$, Fig. 1D, F (1, 54) = 33.88, $P < 0.0001$, Fig. 1F). Further, the swing speed of 6- and 9-m old 5xFAD mice were decreased compared to WT ones (F (1, 54) = 5.383, F (1, 54) = 14.42, $P = 0.0004$, Fig. 1G). For stride length, all paws of 5×FAD mice showed significantly decreased with age, and there is significant difference between 3- and 9-m old groups (F (2, 54) = 3.041, $P = 0.0500$). Compared to 3- and 6-m old WT mice, the four paws stride length of age-matched 5×FAD ones showed only a tendency towards decrease, while there was a significant decrease in 9-m old group (F (1, 54) = 13.63, $P = 0.0005$, Fig. 1G). These results indicated that 5xFAD mice showed decreased speed, cadence as well as stride length and increased number of steps, especially in 9-m old group.

Temporal parameters
The temporal parameters results (Fig. 2A) illustrated that 5xFAD mice showed more stance time (F (2, 54) = 4.156, $P = 0.0210$, F (1, 54) = 27.85, $P < 0.0001$, Fig. 2B), swing time (F (2, 51) = 3.920, $P = 0.0261$, F (2, 52) = 7.716, $P = 0.0012$, Fig. 2C), step cycle time (F (3, 72) = 2.788, $P = 0.047$, F (2, 52) = 1.679, $P = 0.1965$, Fig. 2D) and time for all paws to make the maximum contact to the glass (F (2, 53) = 14.29, $P < 0.0001$, F (2, 53) = 14.29, $P < 0.0001$, Fig. 2E) plate with age, and there were statistical differences between 3- and 9-m 5xFAD groups. Moreover, the 9-m old 5×FAD ones showed much more stance time, swing time and step cycle time of all paws (F (1, 54) = 12.62, $P = 0.0008$, Fig. 2B, F (1, 51) = 19.34, $P < 0.0001$, Fig. 2C, F (1, 54) = 9.209, $P = 0.0037$, Fig. 2D). Relative to their stance time, the 9-m old 5×FAD ones also showed increased time for all paws to make the maximum contact at the glass plate relative to their stance time since the start of the trial (F (1, 53) = 9.852, $P = 0.0028$, F
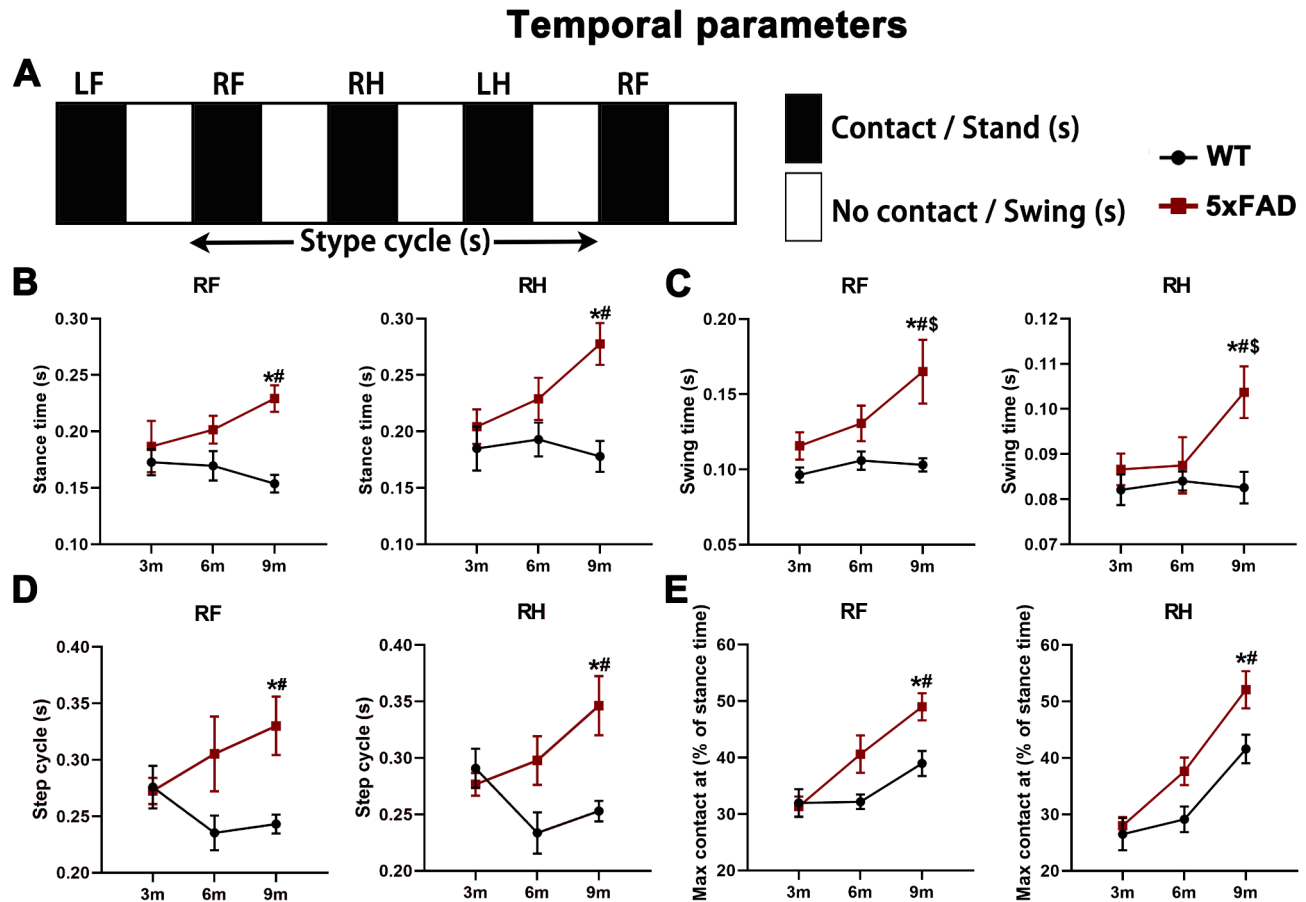
Gait characteristics and kinetic parameters

Fig. 1. The gait characteristics and kinetic parameters of 5xFAD and WT mice. (**A**) Mouse was tested on the runway of Catwalk. (**B**) Weight. (**C**) Average speed. (**D**) Cadence. (**E**) Number of steps. (**F**) Swing speed of right forelimb and hindlimb. (**G**) Stride length of right forelimb and hindlimb. The bars indicate the means ± SEM; $n = 10$ per group; *$p < 0.05$ as compared to the age-matched WT group (Two-way ANOVA and Holm-Sidak test); #$p < 0.05$ as compared to the 3-month-old 5xFAD group (Two-way ANOVA and Holm-Sidak test); $$p < 0.05$ as compared to the 6-month-old 5xFAD group (Two-way ANOVA and Holm-Sidak test).

$(1, 54) = 10.81$, $P = 0.0018$, Fig. 2E). These results suggested that the 5xFAD mice showed significantly increased temporal parameters of all paws at 9-m old.

Spatial parameters

For spatial parameters results (Fig. 3A, B), 5×FAD mice revealed a decreasing trend of print areas (F (2, 54) = 1.231, $P = 0.3002$, F (2, 52) = 16.10, $P < 0.0001$, F (2, 52) = 9.051, $P = 0.0004$, F (2, 53) = 25.03, $P < 0.0001$, Fig. 3C) and maximum intensity (F (2, 54) = 3.868, $P = 0.0269$, F (2, 53) = 9.775, $P = 0.0002$, F (3, 72) = 2.691, $P = 0.05$, F (2, 54) = 6.552, $P = 0.0028$, Fig. 3D) of all paws with age, and the statistic difference between 3- and 9-m old ones was significant. Meanwhile, 9-m old 5×FAD mice showed decreased print areas and maximum intensity of all paws (F (1, 53) = 6.587, $P = 0.0131$, F (1, 52) = 13.37, $P = 0.0006$, F (1, 52) = 12.41, $P = 0.0009$, F (1, 53) = 16.37, $P = 0.0002$, Fig. 3C, F (1, 54) = 20.01, $P < 0.0001$, F (1, 53) = 28.61, $P < 0.0001$, F (1, 54) = 6.586, $P = 0.0131$, F (1, 54) = 6.577, $P = 0.0131$, Fig. 3D). We also discovered the minimum intensity of all paws were highly increased at 9-m old in both WT and 5×FAD groups (F (2, 54) = 28.09, $P < 0.0001$, F (2, 54) = 31.53, $P < 0.0001$, F (2, 54) = 33.17, $P < 0.0001$, F (2, 54) = 27.11, $P < 0.0001$, Fig. 3E), but there was no statistic difference between WT and 5×FAD ones of all ages (F (1, 54) = 0.5942, $P = 0.4442$, F (1, 54) = 0.1190, $P = 0.7315$, F (1, 54) = 0.3375, $P = 0.5637$, F (1, 54) = 0.8395, $P = 0.3636$, Fig. 3E). These results revealed decreased print areas and maximum intensity of all paws in 5×FAD mice.
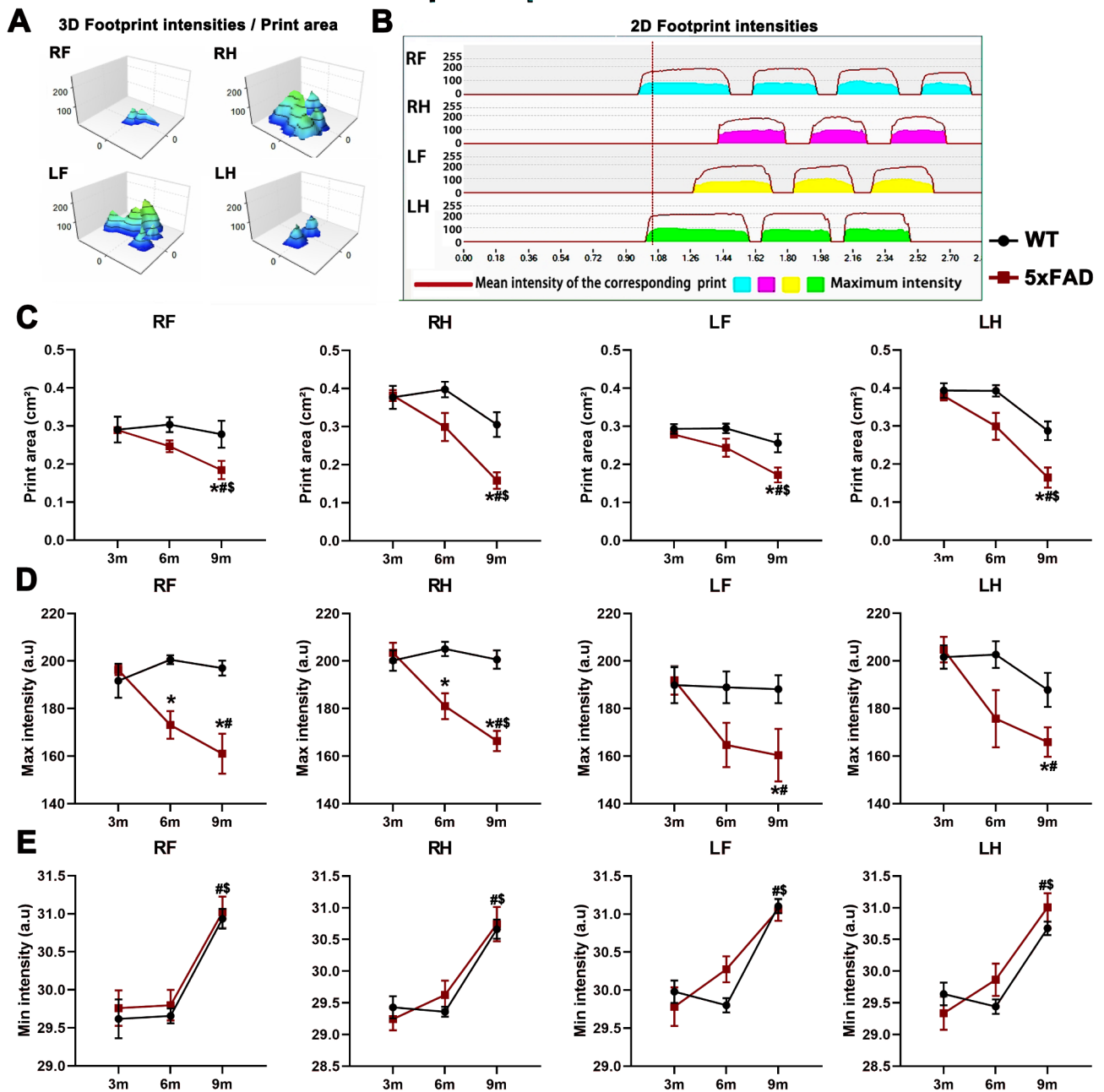
Fig. 2. The temporal parameters of 5xFAD and WT mice. (**A**) Graphical representation of selected gait parameters. (**B**) Stance time of right forelimb and hindlimb. (**C**) Swing time of right forelimb and hindlimb. (**D**) Step cycle time of right forelimb and hindlimb. (**E**) Maximum contact at (% of stance time) of right forelimb and hindlimb. The bars indicate the means ± SEM; $n = 10$ per group; *$p < 0.05$ as compared to the age-matched WT group (Two-way ANOVA and Holm-Sidak test); #$p < 0.05$ as compared to the 3-month-old 5xFAD group (Two-way ANOVA and Holm-Sidak test); $$p < 0.05$ as compared to the 6-month-old 5xFAD group (Two-way ANOVA and Holm-Sidak test).

Interlimb coordination parameters

Comparing interlimb coordination parameters (Fig. 4A) between 5×FAD and WT mice, 5×FAD ones revealed a higher base of support of front and hind paws, and the statistic difference between 9-m old groups was significant ($F_{(1, 50)} = 8.050$, $P = 0.0066$, $F_{(1, 54)} = 13.20$, $P = 0.0006$, Fig. 4B). Due to the increasing tendency of 5xFAD ones with age, the difference in base of support of all paws between 3- and 9-m old groups was significant ($F_{(1, 50)} = 4.34$, $P = 0.0491$, $F_{(2, 54)} = 3.532$, $P = 0.0362$, Fig. 4B). 5xFAD mice also showed significantly reduced print position of both right and left paws with age ($F_{(2, 53)} = 2.593$, $P = 0.0443$, $F_{(2, 53)} = 2.764$, $P = 0.0422$, Fig. 4C)), the difference between 3- and 9-m groups was significant. Meanwhile, 9-m old 5xFAD mice revealed less print position of both right and left paws in comparison with age-matched WT ones ($F_{(1, 53)} = 20.80$ $P < 0.0001$, $F_{(1, 53)} = 22.60$, $P < 0.0001$, Fig. 4C). It was found that WT mice were mainly supported by two paws in a diagonal shape during the trial (about 60%). In contrast, 5×FAD ones revealed a reduced tendency of diagonal shape with age, and there were statistic differences between 3- and 9-m old 5xFAD groups ($F_{(2, 54)} = 3.780$, $P = 0.0291$, $F_{(2, 50)} = 9.616$, $P = 0.0003$, $F_{(2, 51)} = 2.750$, $P = 0.0434$, $F_{(2, 54)} = 2.660$, $P = 0.0491$, $F_{(2, 51)} = 1.742$, $P = 0.4854$, Fig. 4D) and also 9-m old WT and 5xFAD groups ($F_{(1, 54)} = 8.181$, $P = 0.0060$, $F_{(1, 50)} = 5.491$, $P = 0.0231$, $F_{(1, 51)} = 4.779$, $P = 0.0334$, $F_{(1, 54)} = 5.602$, $P = 0.0216$, $F_{(1, 51)} = 4.354$, $P = 0.0419$, Fig. 4D). However, 9-m 5×FAD mice revealed an increased percentage of other types of support patterns, such as girdle, lateral, and even three or four paws with a significant difference (Fig. 4D).

Phase coupling measures inter-paw coordination across girdle, ipsilateral and diagonal paw pairs during spontaneous walk (Fig. 5A)[51]. Increased deviation from expected phase coupling values indicated worsening inter-paw coordination. In comparison with age-matched WT controls, 9-month-old 5xFAD mice displayed a significant increase in phase coupling deviation across most paw pairs ($F_{(1, 53)} = 2.414$, $P = 0.0462$, Fig. 5C, $F_{(1, 51)} = 16.74$, $P = 0.0002$, Fig. 5E, $F_{(1, 52)} = 3.645$, $P = 0.0618$, Fig. 5F, $F_{(1, 52)} = 7.923$, $P = 0.0069$, Fig. 5G). Nevertheless, no significant differences of phase coupling were observed in RF to LF (Fig. 5B) and RH to LH (Fig. 5D). In general, we observed a significant decreasing of inter-paw coordination of 5xFAD mice of all paw
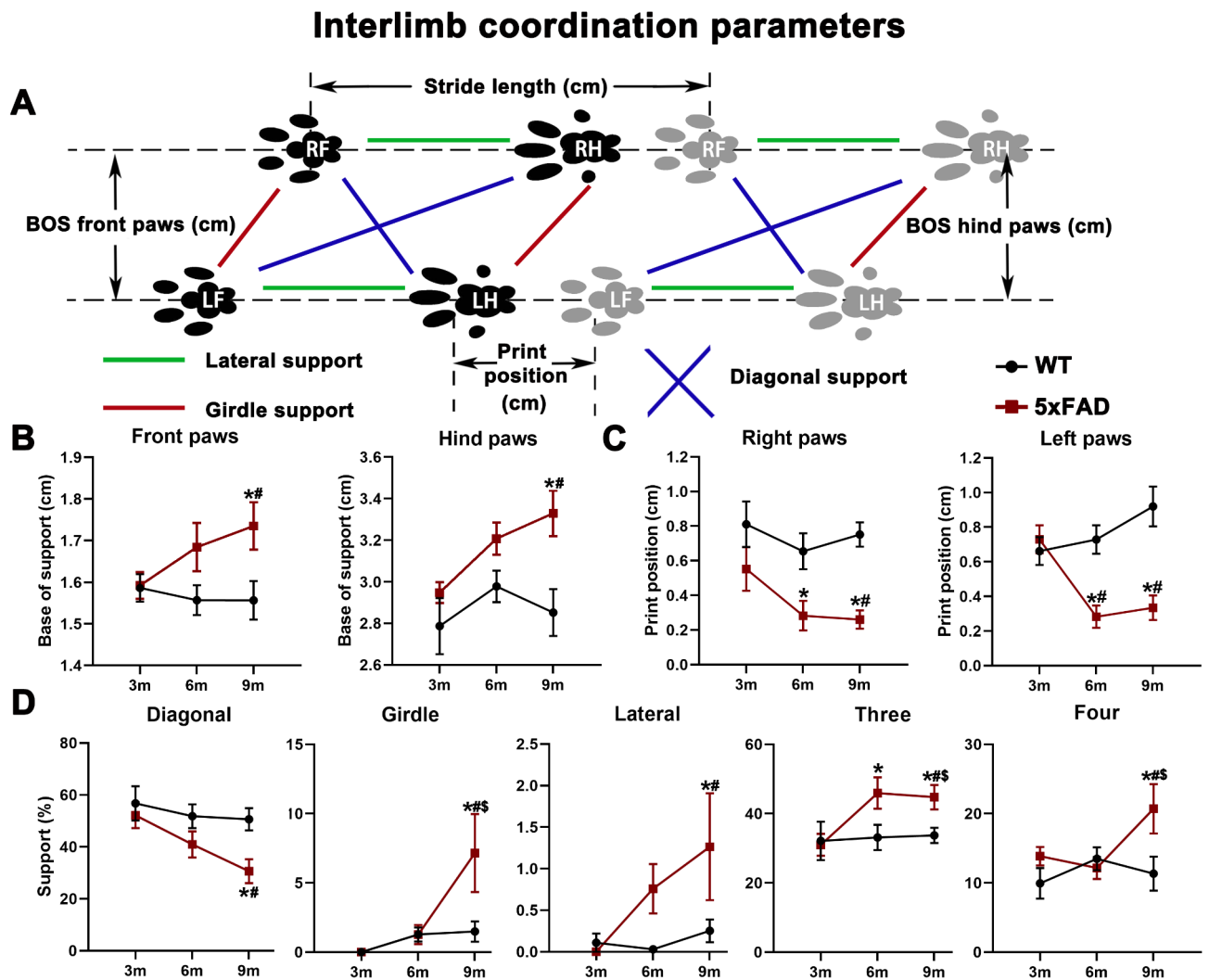
Spatial parameters

Fig. 3. The spatial parameters of 5xFAD and WT mice. (**A**) 3D picture of footprint intensities and print area. (**B**) 2D picture of footprint intensities (**C**) Print area of four limbs. (**D**) Maximum intensity of four limbs. (**E**) Minimum intensity of four limbs. The bars indicate the means ± SEM; $n = 10$ per group; *$p < 0.05$ as compared to the age-matched WT group (Two-way ANOVA and Tukey's test); #$p < 0.05$ as compared to the 3-month-old 5xFAD group (Two-way ANOVA and Tukey's test); $$p < 0.05$ as compared to the 6-month-old 5xFAD group (Two-way ANOVA and Tukey's test).

pairs with aging (F $(1, 52) = 10.15$, $P = 0.0024$, Fig. 5C, F $(2, 51) = 3.874$, $P = 0.0271$, Fig. 5E, F $(2, 52) = 4.804$, $P = 0.0122$, Fig. 5F, F $(2, 52) = 3.109$, $P = 0.050$, Fig. 5G).

For regularity index (Fig. 6A), we discovered that 5xFAD mice showed less and less during the trial with age (F $(2, 54) = 7.507$, $P = 0.0013$, Fig. 6B), and there was significant difference between 3- and 9-m old groups. Compared to age-matched WT mice, the regularity index of 6- and 9-m old 5xFAD ones also decreased significantly (F $(1, 54) = 22.58$, $P < 0.0001$, Fig. 6B). Even no statistic difference was found in the number of footfall patterns between 5xFAD and WT mice of all ages (F $(2, 50) = 0.3552$, $P = 0.7028$, Fig. 6C). But when it comes to gait-pattern frequency distribution, we found that start form 3-m old, compared with age-matched WT mice, 5xFAD ones exhibited a 15 to 20%increase in the frequency of the radial pattern AA (LH-RF-RH-LF)

Fig. 4. The interlimb coordination parameters of 5xFAD and WT mice. (**A**) Graphical representation of selected gait parameters. (**B**) Base of support of front and hind paws. (**C**) Print position of right and left paws. (**D**) Support ways. The bars indicate the means ± SEM; $n = 10$ per group; *$p < 0.05$ as compared to the age-matched WT group (Two-way ANOVA and Holm-Sidak test); #$p < 0.05$ as compared to the 3-month-old 5xFAD group (Two-way ANOVA and Holm-Sidak test); $$p < 0.05$ as compared to the 6-month-old 5xFAD group (Two-way ANOVA and Holm-Sidak test).

(F $(1, 54) = 7.567$, $P = 0.0081$). Meanwhile, the alternating contralateral footfall pattern CB (LH-RH-LF-RF) was used with increased frequency in 5xFAD mice of all ages (F $(1, 54) = 3.957$, $P = 0.05$). Thus, the compensatory adjustments in gait mechanics of 5xFAD mice, observed via gait pattern frequency distribution, revealed that since 3-m old, 5xFAD mice preferentially relied on the AA radial pattern and alternating CB pattern over the AB (LH-LF-RH-RF) (F $(1, 54) = 5.587$, $P = 0.0217$) and CA (LH-RF-LF-RH) (F $(1, 52) = 4.144$, $P = 0.0469$) gait patterns preferentially used by WT mice (Fig. 6D).
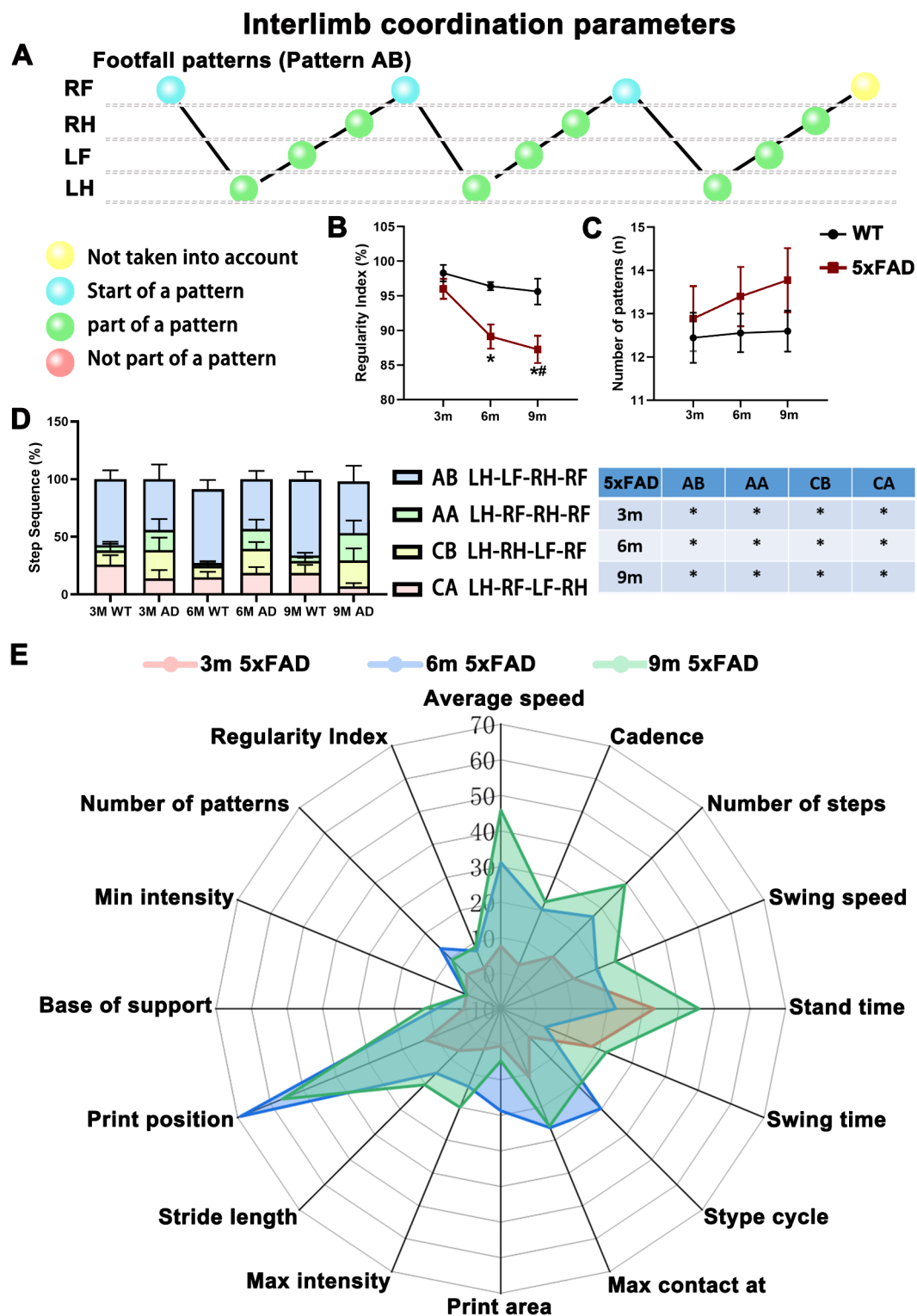
In the end, we use radar plot to illustrate the percentage changes for each gait parameter of 5xFAD mice at different ages in comparison with age-matched WT ones. Not much changes were found between these two groups at 3 months of age, but from 6 months of age, differences started to show in some gait parameters, and by 9 months of age, significant differences were found in all gait parameters apart from the minimum intensity and number of patterns between those two groups (Fig. 6E). These parameters exhibited a significant difference in average speed, cadence, number of steps, stance time, swing time, step cycle time, maximum contact time at the glass plate, print area, maximum intensity, base of support, stride length and regularity index of all paws in average in 5xFAD mice, especially at 9-month-old. Further, we investigated the gait impairment of 9-month-old 5xFAD female mice. While there was no difference in weight (Fig. S2A), the results showed a decrease in average speed (Fig. S2B), cadence (Fig. S2C), swing speed (Fig. S2E) and stride length (Fig. S2F). As well, it shows an increase in the number of steps (Fig. S2D), the time spent in stance (Fig. S2G), the time spent swinging (Fig. S2H), the number of steps per cycle (Fig. S2I), and the maximum contact with the glass plate (Fig. S2J). Also, we found that the base of support (Fig. S2K) and minimum intensity of LH (Fig. S2Q) increased. Additionally, we observed a decrease in print position (Fig. S2L), regularity index (Fig. S2M), print areas (Fig. S2O), and
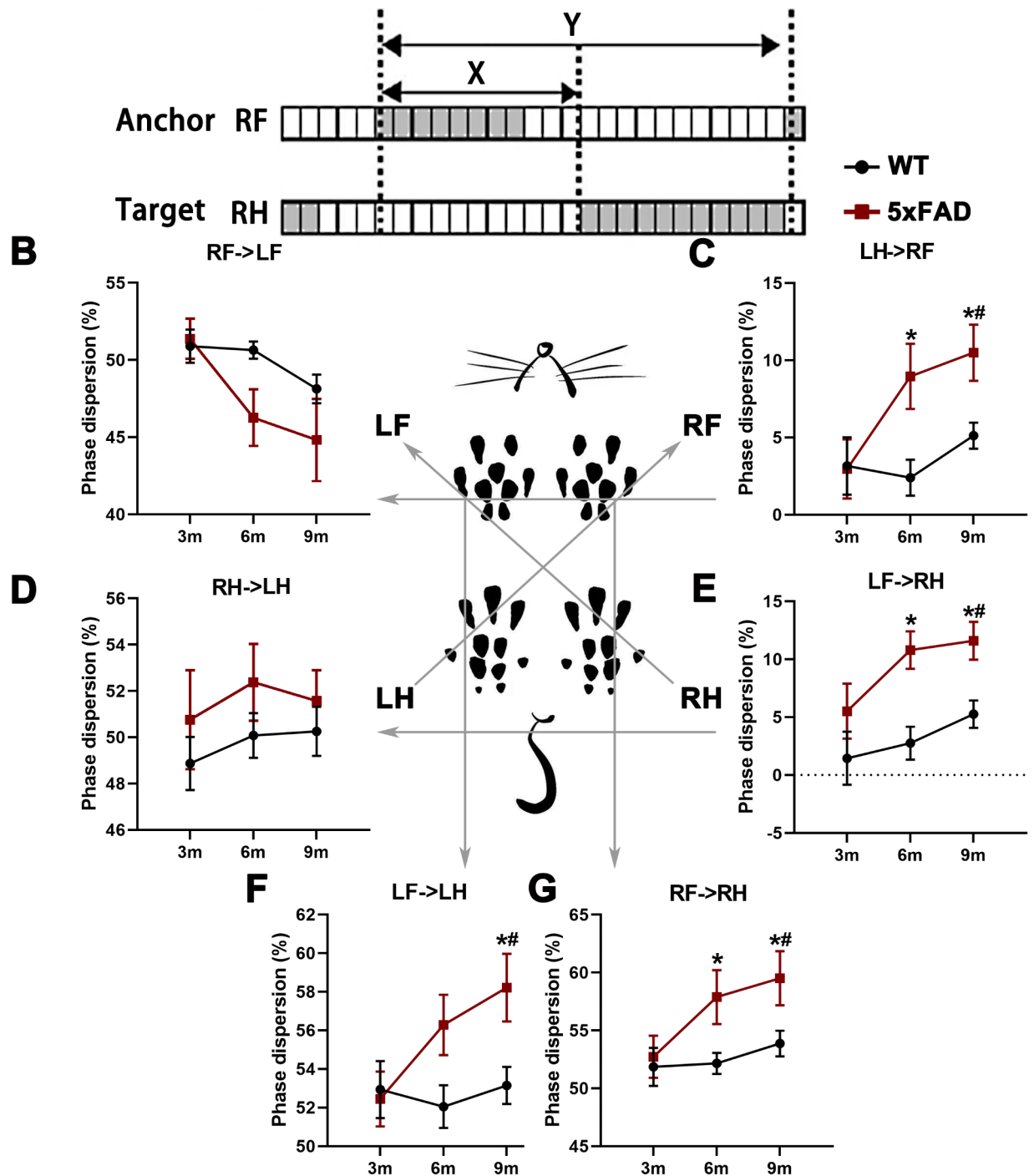
Fig. 5. The Δ phase coupling of 5xFAD and WT mice. (**A**) Graphical representation of phase coupling. (**B**-**G**) Δ Phase coupling of RF to LF (**B**), LH to RF (**C**), RH to LH (**D**), LF to RH (**E**), LF to LH (**F**), RF to RH (**G**). Bar graphs are summary data, indicating that WT mice showed a narrow distribution around the expected value, 5xFAD ones tended to exhibit a more dispersed distribution; $n = 10$ per group; *$p < 0.05$ as compared to the age-matched WT group (Two-way ANOVA and Tukey's test); #$p < 0.05$ as compared to the 3-month-old 5xFAD group (Two-way ANOVA and Tukey's test).

Fig. 6. The footfall patterns and radar plot of gait parameters influenced degree of 5xFAD and WT mice. (**A**) Graphical representation of footfall patterns. (**B**) Regularity index. (**C**) Number of patterns. (**D**) Step sequences. (**E**) Radar plot illustrating the percentage changes for each gait parameter of 5xFAD mice at different ages in comparison with age-matched WT ones. The bars indicate the means ± SEM; $n = 10$ per group; *$p < 0.05$ as compared to the age-matched WT group (Two-way ANOVA and Holm-Sidak test); #$p < 0.05$ as compared to the 3-month-old 5xFAD group (Two-way ANOVA and Holm-Sidak test).

maximum intensity of RF and LH (Fig. S2P). Female 5xFADs exhibiting a reduced tendency for diagonal shape and an increase in three and four-paw support patterns (Fig. S2N). The phase coupling deviation of LH-> RF and LF-> RH increased (Fig. S2R). A similar gait parameter change was found in 9-m female 5xFAD mice, compared to male ones.

Correlation between speed and gait parameters of 5xFAD mice

Based on above results, we found that 5×FAD mice manifested significant functional impairment in gait, especially at the age of 9 months, hence, we focus on the time point of 9-m old for the following study. In addition, in light of findings by Batka et al.[52] and de Haas et al.[53] that CatWalk parameters vary with speed, we decreased this variation by selecting the trials with similar speed for the subsequent analysis of 9-m groups as shown in figure S1 (A-O). It was found that the difference in gait parameters between 5xFAD mice and WT mice disappeared when speeds were the same, suggesting that the difference in gait parameters was the result of a slower speed.

At the same time, we evaluated a possible correlation of every gait parameter of 9-m old 5xFAD mice with speed by calculating linear regression. As illustrated in Fig. 7(all values represented by the average of four paws,) the cadence, stride length, print area, and maximum intensity showed a positive correlation to the speed of mice (Fig. 7A-D). In contrast, base of support, maximum contact time at the glass plate, stand time, number of steps and number of patterns showed a negative correlation to the speed of mice (Fig. 7E-I). While regularity index, step cycle time and swing time showed no significant correlation to the speed of mice (Fig. 7J-L). These results showed a strong correlation between speed and gait parameters, which also highlighted the speed of the mouse as a strong predictor of its gait performance. Furthermore, muscle weakness can contribute to gait impairments. The lack of muscle strength can cause changes in stride length, cadence, and overall stability, which can affect
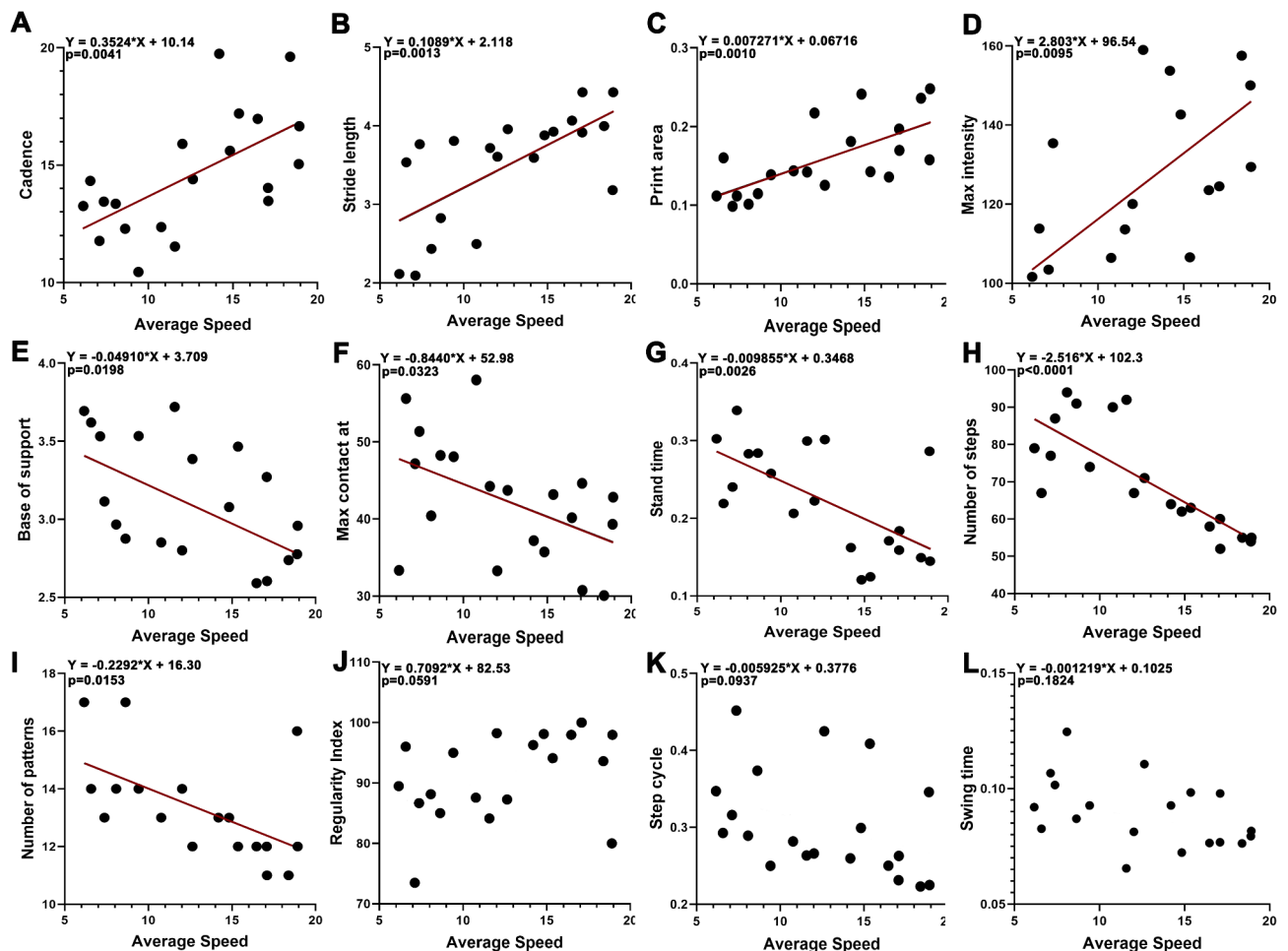
Fig. 7. Correlation between average speed and gait parameters of 9-month-old 5xFAD mice. (**A-D**) The gait parameters (cadence, stride length, print area and max intensity) which are positively correlated with speed. (**E-I**) The gait parameters (base of support, max contact at, stand time, and number of steps) which are negative correlated with speed. (**J-L**) The gait parameters (regularity index, step cycle and swing time) which are not correlated with speed. The average of four paws values was calculated for each parameter and used to plot against corresponding average speed, and it was considered correlated if $p < 0.05$ with linear regression F-test. Significant linear correlations are marked with a red best fit line; $n = 20$.

normal locomotion. Then Forelimb, hindlimb, and wholelimb grip strengths were measured to evaluate muscle function. While, the grip strength showed no significant change compared with the 5xFAD group at 3 (Fig. S3A-C), 6 (Fig. S3D-F), and 9 (Fig. S3G-I) months, or even 9 months for females (Fig. S3J-L). These data suggest that the gait impairments found in 5xFAD were not due to reduced muscle strength.

Impairment of theta oscillations and speed correlated cells in hippocampal CA1 of 5xFAD mice

Then we carried out open field test (OFT) with local field potential (LFP) and single cell activity in vivo recording in the hippocampal CA1 of WT and 5xFAD mice by implanted 32-channel tetrodes. The results are presented below.

The change of theta oscillations in hippocampal CA1 of 5×FAD mice
Firstly, we detected the power spectra of theta rhythm (4–8 Hz)[54,55] at rest and no difference was found between WT and 5xFAD mice. After analyzing the relative power of theta oscillations during locomotor activity, we observed a significant decrease in the relative power of theta oscillations in 5xFAD mice compared with WT ones (Fig. 8A, D). Meanwhile, we found in WT mice the power of theta oscillations was positively correlated with speed, but it seemed no significant correlation between the power of theta oscillations and speed in 5xFAD ones (Fig. 8B, E). Consistent with the gait results, we also found the average speed of 5×FAD mice were significantly reduced compared with WT ones within one trial session of 1500 s (Fig. 8C). These results suggested that the moving speed and power of theta oscillations in the hippocampal CA1 were influenced synchronously in 5×FAD mice compared to WT ones and there might be a causal link between theta rhythm disruption and gait deficits.

The proportion of speed correlated cells changes in hippocampal CA1 of 5×FAD mice
A speed correlated cell (Fig. 9A) was defined by the correlation between firing rates and locomotor speed ($p < 0.05$; linear regression F-test) as described before[56]. We recorded total 114 units in WT and 124 units in transgenic mice. Approximate 60.5% (69/114) units in WT mice (Fig. 9G) and 40.3% (50/124) units (Fig. 9I) in 5xFAD mice showed linearly correlated between single cell spike firing and speed (positive and negative) (Fig. 9B-E). The mean r^2 for a linear speed correlation of all speed cells was 0.31 ± 0.037 in WT mice (0.33 ± 0.033 in 5xFAD); cells with a significant correlation to speed had a mean r^2 of 0.62 ± 0.033 (0.63 ± 0.027 in 5xFAD); and non-significantly correlated cells had an r^2 mean of 0.08 ± 0.015 (0.22 ± 0.027 in 5xFAD) (Fig. 9F, H). These results revealed that there were speed cells in both WT and 5xFAD mice, but the proportion in WT mice was much higher than that in 5xFAD ones.

Discussion

This study demonstrated that the gait differences between 5xFAD mice and WT were increasingly apparent with age, especially in decreased average, body, and swing speed, increased temporal parameters, and reduced spatial ones. The freely moving 9-month-old 5xFAD mice displayed significant changes in their gait signatures, highlighting the aspects of gait changes observed in AD patients, including changes in speed, cadence, gait variability, footfall pattern distribution, etc., compared with age-matched controls[57]. Particularly, the reduced print areas of all paws in aged 5xFAD mice may indicate an incomplete stance of the paws during locomotion, which could lead to a reduction in the efficiency of every step[58,59], suggesting a less efficient walking style than in normal mice. The lower maximum intensity of all paws in aged 5xFAD mice compared with WT ones indicated their decreased propulsion[60], showing the feebleness of 5xFAD mice. Moreover, the reduced average, body, and swing speeds of 5xFAD mice could negatively impact coordination.

Therefore, factors associated with coordination are of particular significance, as interlimb coordination is crucial for locomotion. The most frequently used synchronized paw pair during floor contact was two diagonal paws (60%) for a large percentage of normal control mice. However, apart from the decreased frequency of diagonal support in aged 5xFAD mice, all other forms of paw support increased compared to WT mice, suggesting that the stability of 5xFAD mice was significantly compromised[61,62].

Further, the deterioration of locomotor coordination in 5xFAD mice was also assessed by analyzing the extent of synchrony between diagonal, horizontal, and lateral limb couplets in each group, a procedure also known as phase coupling. Inter-limb coupling was examined by computing the interval between the onset times of each paw in a pair contacting the ground. The absolute difference between the actual and expected coupling values was analyzed as an asynchrony index[63]. For example, the expected interlimb coupling value is zero if the diagonal limbs are moving in synchrony. It is widely recognized that horizontal pairs of extremities alter more frequently than diagonal pairs when walking. When the two extremities are precisely swapped, the inter-limb coupling value is 50%[47,64]. In the current study, compared with WT ones, increased deviation of 9-month-old 5xFAD mice from expected phase coupling values suggests worsening inter-paw coordination which is also commonly shown in AD patients[53].

The four most prevalent step-sequence patterns in rodents are AB, AA, CB, and CA. These patterns change due to stress or motor diseases[65,66]. This study demonstrated that the primary step sequence pattern (AB) was consistent across all ages of WT mice, consistent with a previous report. Intact rodents preferred this regular step pattern in 80–95% of cases[67]. However, in this study, the AB pattern was reduced in 5xFAD mice as young as three months, while the frequency of the radial pattern AA, also known as the "giraffe walk," increased by 15 to 20%[68]. This gait pattern was elevated in aged people[69] and mouse models with increased gait instability[70]. These results highlight the significant deficiency of 5xFAD mice in interlimb coordination which is consistent with AD patients[71,72].

Since locomotion speed influences four distinct movement metrics, the statistical analysis indicates intra- and inter-individual variability[47,52,73]. Our results demonstrated that the decreased speed observed in
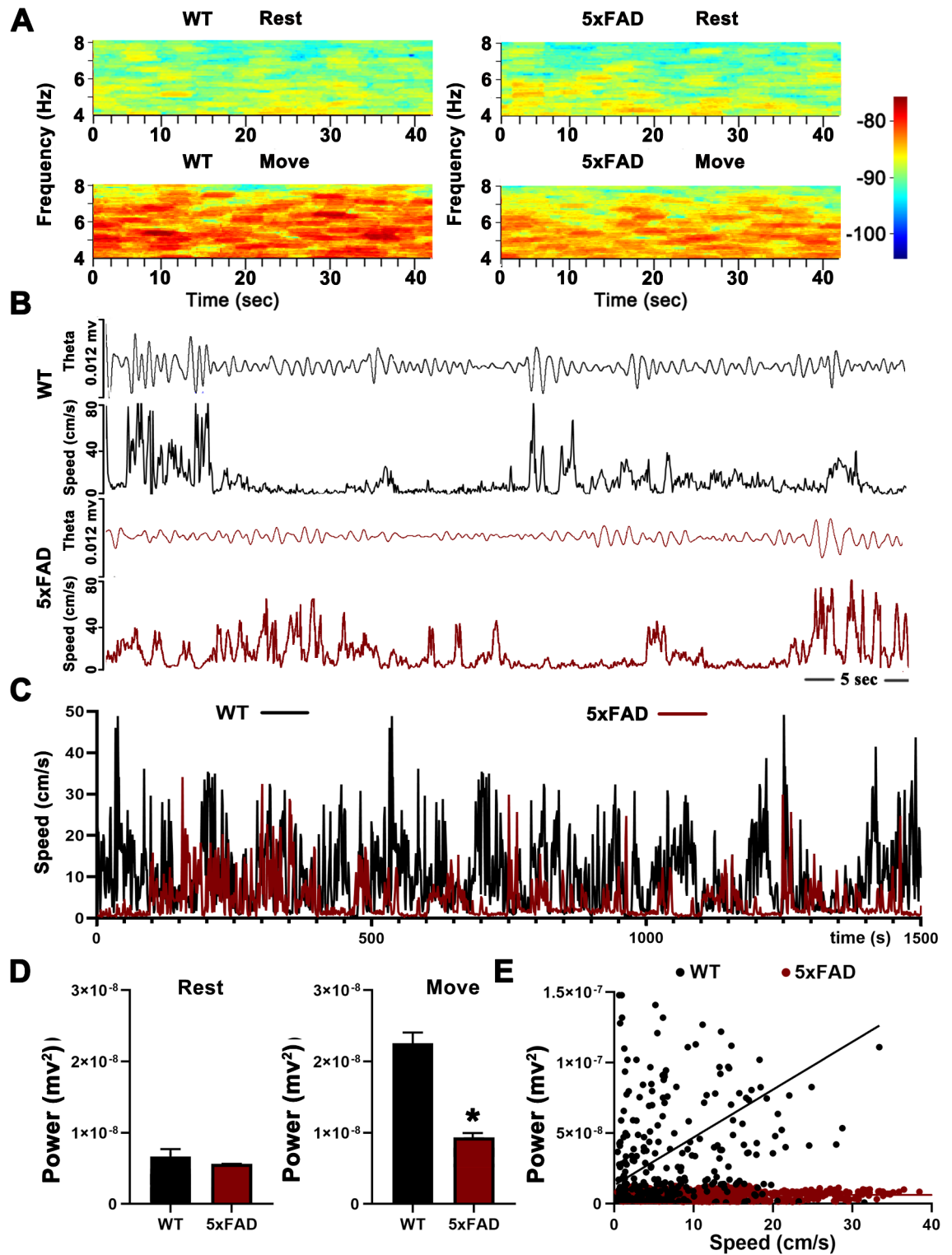
Fig. 8. The change of speed and theta oscillations in hippocampal CA1. (**A**) Representative power spectrogram of theta frequency from WT and 5xFAD mice at rest and move. (**B**) Representative speed plot and corresponding filtered theta component of the signal from WT and 5xFAD mice in OFT. (**C**) The average speed of WT and 5xFAD mice. (**D**) The power of theta oscillations at rest and during locomotor activity. (**E**) The correlation between speed and corresponding theta power in hippocampal CA1 during locomotor activity (WT: $Y = 1.417e\text{-}009*X + 1.371e\text{-}008$; $p < 0.05$; 5xFAD: $Y = 9.183e\text{-}012*X + 6.080e\text{-}009$; $p = 0.248$; linear regression F-test). The bars indicate the means $\pm$ SEM; $n = 5$ per group; $^*p < 0.05$ (Unpaired t test).
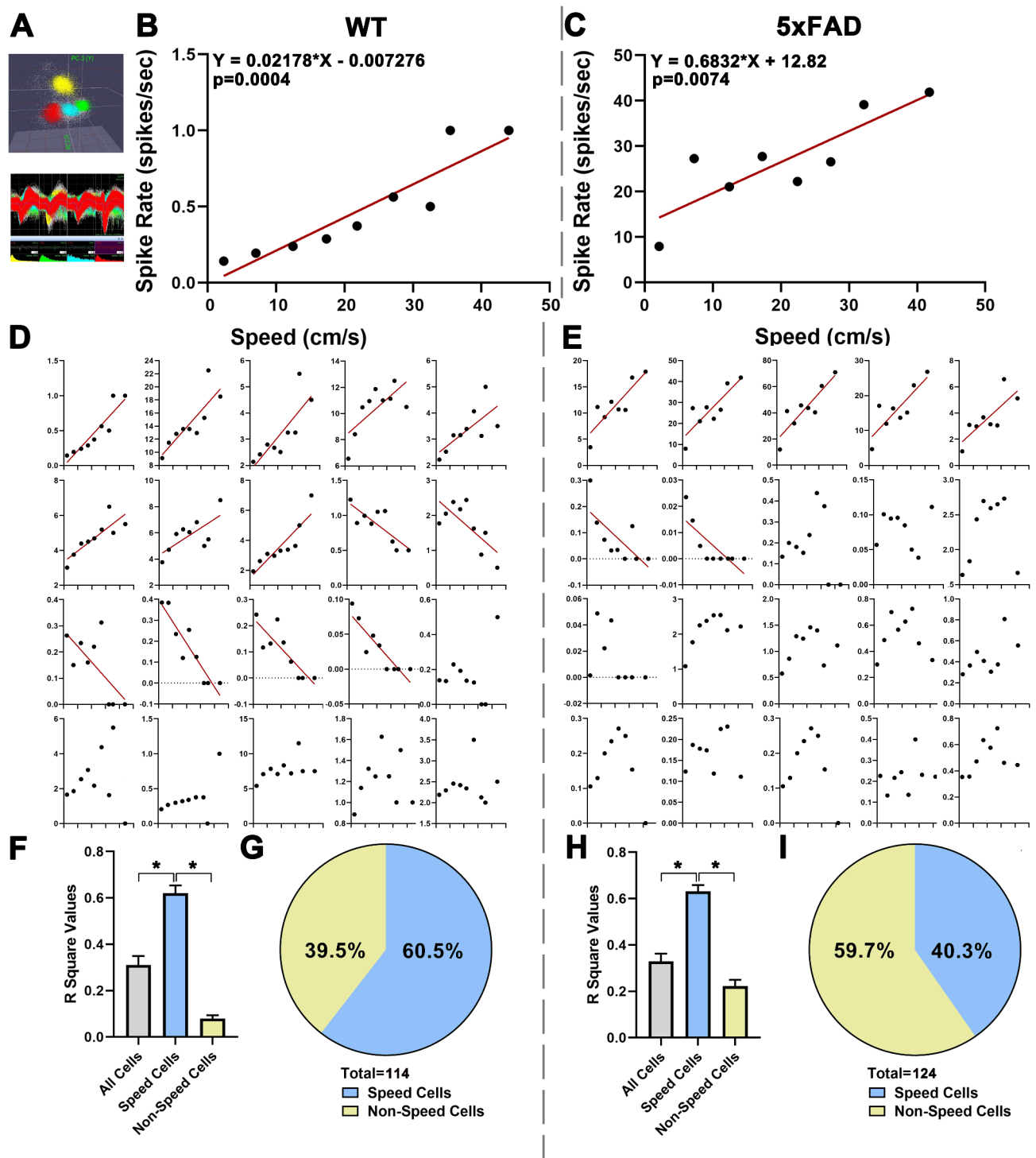
Fig. 9. The change of speed cells proportion in hippocampal CA1. (**A**) Spike Sorting for different neurons. (**B**) An example of speed correlated cell in WT mouse. (**C**) Same as (**B**) but the mouse is 5xFAD.(**D**) The speed correlations for all cells in hippocampal CA1 of WT mouse in one session of OFT and cell was considered correlated if $p < 0.05$ (linear regression F-test). Significant linear correlations are marked with a red best fit line. (**E**) Same as (**D**) but the mouse is 5xFAD. (**F,H**) Mean r^2 values for all cells, speed cells, and non-speed cells in hippocampal CA1 of WT and 5xFAD mice. (**G, I**) Diagram showing the proportions of speed cells and non-speed cells in hippocampal CA1 of WT and 5xFAD mice. (A speed cell was defined by the correlation between firing rates and running speed [$p < 0.05$; linear regression F-test]. Significant linear correlations are marked with a red best fit line. The bars indicate the means ± SEM; $n = 5$ per group; *$p < 0.05$ (Unpaired t test).

9-month-old 5xFAD mice is likely a significant factor contributing to their impaired gait behavior compared to WT mice. Several studies have indicated that the speed of adult mice influences various gait parameters in quadruples, resulting in intra and inter-individual variability that are invisible in the statistical analysis[47,73,74]. Another comprehensive study was conducted on 16 WT mice to investigate the relationship between speed and 162 locomotion parameters reported by the CatWalk software. The results indicated that over 90% of these parameters were speed-dependent[52].

Evidence suggests a strong correlation between gait variability in AD patients and structural and functional alterations in the hippocampus[72,75,76]. Thus, abnormal hippocampal function may significantly impact gait and its well-known effects on learning and memory. One of the most prominent topics to study about hippocampus dysfunction is theta oscillations, which shows intriguing correlations with different behaviors that include both movement and memory function[41]. Theta rhythm is related to other types of movement behaviors, including running on a treadmill[77], track[78], and running wheel[79]. Similarly, theta rhythm correlates with learning and memory functions[80]. Theta rhythm has been related to arousal[81], attention[82], and sensorimotor integration[83], even though it has been less extensively investigated than movement and memory correlates. Shin suggested that theta oscillations could encode motor behavior data[84]. Meanwhile, multiple studies have demonstrated a positive correlation between the frequency and amplitude of theta rhythm in the field potential of hippocampal CA1 and locomotor speed[33,85-87]. This correlation can be observed across three simultaneous recording sites in CA1[88]. Further, optogenetically increasing the amplitude of theta oscillations in hippocampal CA1 increased locomotion speed[89], indicating that the hippocampal theta rhythm plays a critical role in the coding of locomotion velocity. Impaired theta oscillations in the hippocampal CA1 region was considered one of the causes of impaired hippocampal-dependent cognitive function in AD rats[90] and 5xFAD mice[91]. Based on our results, theta oscillations in the hippocampal CA1 were substantially reduced during locomotor activity compared to the WT controls. This explains the slower speed observed in 5×FAD mice and the subsequent gait impairment.

The hippocampus has long been associated with memory and learning; however, evidence shows it is also involved in locomotion regulation[83]. Thus far, speed modulation has mainly been reported in the hippocampal CA1 and the medial entorhinal cortex (MEC) in combination with positional information or as a non-conjunctive code (speed cells)[29,30]. Neurons that encode for speed have been previously identified in the medial entorhinal cortex[92,93] and have been more recently investigated in the hippocampus[29,94]. This is consistent with previous findings. The hippocampus's neurons have been demonstrated to manifest spiking activity associated with speed[95,96]. To understand the reason for the decline in speed of 5xFAD mice, our study explored the relationship between speed cells and speed using tetrode in vivo recording of the hippocampal CA1. This allowed us to investigate whether the decrease in speed observed in 5xFAD mice was associated with a reduction in the proportion of speed cells. Our results confirmed and expanded upon previous reports by demonstrating that (1) speed cells were present in the hippocampal CA1, (2) the firing rate of CA1 neurons was a stable indicator of speed, and (3) the number of CA1 speed cells in WT mice was greater than that in 5xFAD mice. Despite the hippocampus being associated with memory and learning, the current experiments suggest a strong correlation with the sensory-motor system. However, these results need to be confirmed, and the mechanism of speed cells in the hippocampal region has yet to be known. It has also been shown that the spiking activity of hippocampal neurons oscillates at theta frequency, which is influenced by the LFP theta phase[97,98]. After that, the "oscillatory coding" effect could be observed as a correlation between fluctuations in the firing rate of CA1 speed cells and variations in theta frequency with speed. Specifically, a higher frequency of theta cycles would lead to a greater number of spikes per unit of time[94]. Simultaneously, the findings suggest that neurons in the hippocampal formation and entorhinal cortex directly code locomotor speed with changes in firing rate[94,99]. Locomotor speed can be encoded by various types of neurons, such as grid cells and head direction cells in the hippocampus, CA1[100]. The frequency of these speed cells typically increases as the speed increases[37,101]. The current study discovered a population of speed cells in the hippocampal CA1. These cells show a direct correlation between their activity and locomotor speed in the WT and 5xFAD groups, similar to previous research. In the hippocampal CA1 of 5xFAD mice, speed cells were decreased compared to the normal control group. This reduction in speed cells may be a factor in the overall decline in speed.

In conclusion, this study characterized the age-related variations in the voluntary walking gait performance of male 5xFAD mice. Meanwhile, 5xFAD mice demonstrated quantifiable, clinically significant changes in gait function when examined with age-matched WT mice at 9 months of age, which underscores the findings in human AD patients. Furthermore, it is possible that the abnormal operation of the hippocampal CA1, including attenuated theta oscillation power and decreased proportion of speed cells could have been responsible for all the impaired gaits.

Data availability

References

1. Leisman, G., Moustafa, A. A. & Shafir, T. Thinking, walking, talking: integratory motor and cognitive brain function. *Front. Public. Health.* **4**, 94 (2016).
2. Pirker, W. & Katzenschlager, R. Gait disorders in adults and the elderly: A clinical guide. *Wien Klin. Wochenschr.* **129** (3–4), 81–95 (2017).
3. Montgomery, G. et al. Determinants of performance in the timed Up-and-Go and Six-Minute walk tests in young and old healthy adults. *J. Clin. Med.* **9**(5). (2020).

4. Lemieux, M. et al. Speed-Dependent modulation of the locomotor behavior in adult mice reveals attractor and transitional gaits. *Front. Neurosci.* **10**, 42 (2016).
5. Scheltens, P. et al. *Alzheimer's Disease Lancet*, **397**(10284): 1577–1590. (2021).
6. Webster, K. E., Merory, J. R. & Wittwer, J. E. Gait variability in community dwelling adults with alzheimer disease. *Alzheimer Dis. Assoc. Disord.* **20** (1), 37–40 (2006).
7. Nadkarni, N. K. et al. Gait and subcortical hyperintensities in mild Alzheimer's disease and aging. *Dement. Geriatr. Cogn. Disord.* **28** (4), 295–301 (2009).
8. Koppelmans, V., Silvester, B. & Duff, K. Neural mechanisms of motor dysfunction in mild cognitive impairment and Alzheimer's disease: A systematic review. *J. Alzheimers Dis. Rep.* **6** (1), 307–344 (2022).
9. Lin, Y. C. et al. Comparison of motor performance of upper and lower extremities in dual-task tests in patients with mild Alzheimer's dementia. *Aging Clin. Exp. Res.* **28** (3), 491–496 (2016).
10. Fritz, N. E. et al. Motor performance differentiates individuals with lewy body dementia, Parkinson's and Alzheimer's disease. *Gait Posture.* **50**, 1–7 (2016).
11. Min, J. Y. et al. Use of electroencephalogram, gait, and their combined signals for classifying cognitive impairment and normal cognition. *Front. Aging Neurosci.* **14**, 927295 (2022).
12. Bovonsunthonchai, S. et al. Quantitative gait analysis in mild cognitive impairment, dementia, and cognitively intact individuals: a cross-sectional case-control study. *BMC Geriatr.* **22** (1), 767 (2022).
13. Mc Ardle, R. et al. What can quantitative gait analysis tell us about dementia and its subtypes?? A structured review. *J. Alzheimers Dis.* **60** (4), 1295–1312 (2017).
14. Gabell, A. & Nayak, U. S. The effect of age on variability in gait. *J. Gerontol.* **39** (6), 662–666 (1984).
15. Lord, S. et al. Gait variability in older adults: a structured review of testing protocol and clinimetric properties. *Gait Posture.* **34** (4), 443–450 (2011).
16. Pieruccini-Faria, F. et al. Gait variability across neurodegenerative and cognitive disorders: results from the Canadian consortium of neurodegeneration in aging (CCNA) and the gait and brain study. *Alzheimers Dement.* **17** (8), 1317–1328 (2021).
17. Higuma, M. et al. Whole-Day gait monitoring in patients with Alzheimer's disease: A relationship between attention and gait cycle. *J. Alzheimers Dis. Rep.* **1** (1), 1–8 (2017).
18. Bridenbaugh, S. A. & Kressig, R. W. Motor cognitive dual tasking: early detection of gait impairment, fall risk and cognitive decline. *Z. Gerontol. Geriatr.* **48** (1), 15–21 (2015).
19. Cicirelli, G. et al. Human gait analysis in neurodegenerative diseases: A review. *IEEE J. Biomed. Health Inf.* **26** (1), 229–242 (2022).
20. Timotius, I. K. et al. Systematic data analysis and data mining in catwalk gait analysis by heat mapping exemplified in rodent models for neurodegenerative diseases. *J. Neurosci. Methods.* **326**, 108367 (2019).
21. Walter, J. et al. The catwalk XT(R) is a valid tool for objective assessment of motor function in the acute phase after controlled cortical impact in mice. *Behav. Brain Res.* **392**, 112680 (2020).
22. Garrick, J. M. et al. Evaluating gait and locomotion in rodents with the catwalk. *Curr. Protoc.* **1** (8), e220 (2021).
23. Crowley, S. T., Kataoka, K. & Itaka, K. Combined catwalk index: an improved method to measure mouse motor function using the automated gait analysis system. *BMC Res. Notes.* **11** (1), 263 (2018).
24. O'Leary, T. P. et al. Motor function deficits in the 12 month-old female 5xFAD mouse model of Alzheimer's disease. *Behav. Brain Res.* **337**, 256–263 (2018).
25. Oblak, A. L. et al. Comprehensive evaluation of the 5XFAD mouse model for preclinical testing applications: A MODEL-AD study. *Front. Aging Neurosci.* **13**, 713726 (2021).
26. Seo, J. S. et al. Severe motor neuron degeneration in the spinal cord of the Tg2576 mouse model of alzheimer disease. *J. Alzheimers Dis.* **21** (1), 263–276 (2010).
27. Stover, K. R. et al. Analysis of motor function in 6-month-old male and female 3xTg-AD mice. *Behav. Brain Res.* **281**, 16–23 (2015).
28. Jones, M. W. & Wilson, M. A. Theta rhythms coordinate hippocampal-prefrontal interactions in a Spatial memory task. *PLoS Biol.* **3** (12), e402 (2005).
29. Kropff, E. et al. Speed cells in the medial entorhinal cortex. *Nature* **523** (7561), 419–424 (2015).
30. Hardcastle, K. et al. A multiplexed, heterogeneous, and adaptive code for navigation in medial entorhinal cortex. *Neuron* **94** (2), 375–387e7 (2017).
31. Buzsaki, G. Theta oscillations in the hippocampus. *Neuron* **33** (3), 325–340 (2002).
32. Gu, Z. et al. Hippocampus and entorhinal cortex recruit cholinergic and NMDA receptors separately to generate hippocampal theta oscillations. *Cell. Rep.* **21** (12), 3585–3595 (2017).
33. Jeewajee, A. et al. Grid cells and theta as oscillatory interference: electrophysiological data from freely moving rats. *Hippocampus* **18** (12), 1175–1185 (2008).
34. Geisler, C. et al. Hippocampal place cell assemblies are speed-controlled oscillators. *Proc. Natl. Acad. Sci. U. S. A.* **104** (19), 8149–8154 (2007).
35. Spalla, D., Treves, A. & Boccara, C. N. Angular and linear speed cells in the parahippocampal circuits. *Nat Commun* **13** (1) p. 1907. (2022).
36. Kim, J. et al. Gallotannin-Capped gold nanoparticles: green synthesis and enhanced morphology of AFM images. *J. Nanosci. Nanotechnol.* **16** (6), 5991–5998 (2016).
37. Stensola, H. et al. The entorhinal grid map is discretized. *Nature* **492** (7427), 72–78 (2012).
38. Baik, K. et al. Implication of EEG theta/alpha and theta/beta ratio in Alzheimer's and lewy body disease. *Sci. Rep.* **12** (1), 18706 (2022).
39. Jeong, J. EEG dynamics in patients with Alzheimer's disease. *Clin. Neurophysiol.* **115** (7), 1490–1505 (2004).
40. Bennys, K. et al. Diagnostic value of quantitative EEG in Alzheimer's disease. *Neurophysiol. Clin.* **31** (3), 153–160 (2001).
41. Korotkova, T. et al. Reconciling the different faces of hippocampal theta: the role of theta oscillations in cognitive, emotional and innate behaviors. *Neurosci. Biobehav Rev.* **85**, 65–80 (2018).
42. Lu, L. et al. Control of locomotor speed, arousal, and hippocampal theta rhythms by the nucleus incertus. *Nat. Commun.* **11** (1), 262 (2020).
43. Yang, Y. et al. Genetic model of selective COX2 Inhibition improve learning and memory ability and brain pathological changes in 5xFAD mouse. *Brain Res.* **1821**, 148566 (2023).
44. Oakley, H. et al. Intraneuronal beta-amyloid aggregates, neurodegeneration, and neuron loss in transgenic mice with five familial Alzheimer's disease mutations: potential factors in amyloid plaque formation. *J. Neurosci.* **26** (40), 10129–10140 (2006).
45. Jawhar, S. et al. Motor deficits, neuron loss, and reduced anxiety coinciding with axonal degeneration and intraneuronal Abeta aggregation in the 5XFAD mouse model of Alzheimer's disease. *Neurobiol. Aging.* **33** (1), 196e29–196e40 (2012).
46. Ungvari, Z. et al. Cerebromicrovascular dysfunction predicts cognitive decline and gait abnormalities in a mouse model of whole brain irradiation-induced accelerated brain senescence. *Geroscience* **39** (1), 33–42 (2017).
47. Caballero-Garrido, E. et al. Characterization of long-term gait deficits in mouse dMCAO, using the catwalk system. *Behav. Brain Res.* **331**, 282–296 (2017).
48. Kloos, A. D. et al. Stepwise motor and all-or-none sensory recovery is associated with nonlinear sparing after incremental spinal cord injury in rats. *Exp. Neurol.* **191** (2), 251–265 (2005).

49. Nyul-Toth, A. et al. Early manifestation of gait alterations in the Tg2576 mouse model of Alzheimer's disease. *Geroscience* **43** (4), 1947–1957 (2021).

50. Song, D. et al. The lateralization of left hippocampal CA3 during the retrieval of spatial working memory. *Nat. Commun.* **11** (1), 2901 (2020).

51. Chen, Y. J. et al. Detection of subtle neurological alterations by the catwalk XT gait analysis system. *J. Neuroeng. Rehabil.* **11**, 62 (2014).

52. Batka, R. J. et al. The need for speed in rodent locomotion analyses. *Anat. Rec (Hoboken)*. **297** (10), 1839–1864 (2014).

53. de Haas, R., Russel, F. G. & Smeitink, J. A. Gait analysis in a mouse model resembling Leigh disease. *Behav. Brain Res.* **296**, 191–198 (2016).

54. Engel, A. K., Fries, P. & Singer, W. Dynamic predictions: oscillations and synchrony in top-down processing. *Nat. Rev. Neurosci.* **2** (10), 704–716 (2001).

55. Goodman, M. S. et al. Theta-Gamma coupling and working memory in Alzheimer's dementia and mild cognitive impairment. *Front. Aging Neurosci.* **10**, 101 (2018).

56. Wirtshafter, H. S. & Wilson, M. A. Locomotor and hippocampal processing converge in the lateral septum. *Curr. Biol.* **29** (19), 3177–3192 (2019). e3.

57. Castillo-Mariqueo, L. & Gimenez-Llort, L. *Clasping, Ledge-score Coordination and Early Gait Impairments as Primary Behavioural Markers of Functional Impairment in Alzheimer's Disease. Behav. Brain Res.*, p. 114054. (2022).

58. Hamlin, M. et al. A novel device for studying weight supported, quadrupedal overground locomotion in spinal cord injured rats. *J. Neurosci. Methods*. **246**, 134–141 (2015).

59. Omana, H., Madou, E. & Hunter, S. W. The effects on gait of 4-wheeled walker use in people with Alzheimer's disease dementia and gait impairment: A pilot study (J Alzheimers Dis, 2022).

60. Hetze, S. et al. Gait analysis as a method for assessing neurological outcome in a mouse model of stroke. *J. Neurosci. Methods*. **206** (1), 7–14 (2012).

61. Pitzer, C., Kurpiers, B. & Eltokhi, A. Gait performance of adolescent mice assessed by the catwalk XT depends on age, strain and sex and correlates with speed and body weight. *Sci. Rep.* **11** (1), 21372 (2021).

62. Heinzel, J. et al. Use of the catwalk gait analysis system to assess functional recovery in rodent models of peripheral nerve injury - a systematic review. *J. Neurosci. Methods*. **345**, 108889 (2020).

63. Frohlich, H. et al. A machine learning approach to automated gait analysis for the Noldus catwalk system. *IEEE Trans. Biomed. Eng.* **65** (5), 1133–1139 (2018).

64. Mc Ardle, R. et al. Do Alzheimer's and lewy body disease have discrete pathological signatures of gait? *Alzheimers Dement.* **15** (10), 1367–1377 (2019).

65. Herold, S. et al. CatWalk gait analysis in a rat model of multiple sclerosis. *BMC Neurosci.* **17** (1), 78 (2016).

66. Hamers, F. P. et al. Automated quantitative gait analysis during overground locomotion in the rat: its application to spinal cord contusion and transection injuries. *J. Neurotrauma*. **18** (2), 187–201 (2001).

67. Cheng, H. et al. Gait analysis of adult paraplegic rats after spinal cord repair. *Exp. Neurol.* **148** (2), 544–557 (1997).

68. Tarantini, S. et al. Age-Related alterations in gait function in freely moving male C57BL/6 mice: translational relevance of decreased Cadence and increased gait variability. *J. Gerontol. Biol. Sci. Med. Sci.* **74** (9), 1417–1421 (2019).

69. Vestergaard, S. et al. Characteristics of 400-meter walk test performance and subsequent mortality in older adults. *Rejuvenation Res.* **12** (3), 177–184 (2009).

70. Maricelli, J. W. et al. Trendelenburg-Like gait, instability and altered step patterns in a mouse model for limb girdle muscular dystrophy 2i. *PLoS One*. **11** (9), e0161984 (2016).

71. Cedervall, Y., Halvorsen, K. & Aberg, A. C. A longitudinal study of gait function and characteristics of gait disturbance in individuals with Alzheimer's disease. *Gait Posture*. **39** (4), 1022–1027 (2014).

72. Beauchet, O. et al. Association of hippocampal volume with gait variability in pre-dementia and dementia stages of alzheimer disease: results from a cross-sectional study. *Exp. Gerontol.* **115**, 55–61 (2019).

73. Parkkinen, S. et al. Gait impairment in a rat model of focal cerebral ischemia. *Stroke Res. Treat.* **2013**, p410972 (2013).

74. Gorska, T., Zmyslowski, W. & Majczynski, H. Overground locomotion in intact rats: interlimb coordination, support patterns and support phases duration. *Acta Neurobiol. Exp. (Wars)*. **59** (2), 131–144 (1999).

75. Beauchet, O. et al. Hippocampal volume, early cognitive decline and gait variability: which association? *Exp. Gerontol.* **61**, 98–104 (2015).

76. Tian, Q. et al. The brain map of gait variability in aging, cognitive impairment and dementia-A systematic review. *Neurosci. Biobehav Rev.* **74(Pt A)**, p149–162 (2017).

77. Brankack, J., Stewart, M. & Fox, S. E. Current source density analysis of the hippocampal theta rhythm: associated sustained potentials and candidate synaptic generators. *Brain Res.* **615** (2), 310–327 (1993).

78. Skaggs, W. E. et al. Theta phase precession in hippocampal neuronal populations and the compression of Temporal sequences. *Hippocampus* **6** (2), 149–172 (1996).

79. Hyman, J. M. et al. Stimulation in hippocampal region CA1 in behaving rats yields long-term potentiation when delivered to the peak of theta and long-term depression when delivered to the trough. *J. Neurosci.* **23** (37), 11725–11731 (2003).

80. Griffin, A. L. et al. Theta-contingent trial presentation accelerates learning rate and enhances hippocampal plasticity during trace eyeblink conditioning. *Behav. Neurosci.* **118** (2), 403–411 (2004).

81. Green, J. D. & Arduini, A. A. Hippocampal electrical activity in arousal. *J. Neurophysiol.* **17** (6), 533–557 (1954).

82. Michel, R., Dugue, L. & Busch, N. A. Distinct contributions of alpha and theta rhythms to perceptual and attentional sampling. *Eur. J. Neurosci.* **55** (11–12), 3025–3039 (2022).

83. Bland, B. H. & Oddie, S. D. Theta band Oscillation and synchrony in the hippocampal formation and associated structures: the case for its role in sensorimotor integration. *Behav. Brain Res.* **127** (1–2), 119–136 (2001).

84. Shin, J. & Talnov, A. A single trial analysis of hippocampal theta frequency during nonsteady wheel running in rats. *Brain Res.* **897** (1–2), 217–221 (2001).

85. Abubaker, M., Qasem, W. A. & Kvasnak, E. Working memory and cross-frequency coupling of neuronal oscillations. *Front. Psychol.* **12**, 756661 (2021).

86. Ning, W., Bladon, J. H. & Hasselmo, M. E. Complementary representations of time in the prefrontal cortex and hippocampus. *Hippocampus* **32** (8), 577–596 (2022).

87. Jeewajee, A. et al. Theta phase precession of grid and place cell firing in open environments. *Philos. Trans. R Soc. Lond. B Biol. Sci.* **369** (1635), 20120532 (2014).

88. Hinman, J. R. et al. Septotemporal variation in dynamics of Theta: speed and habituation. *J. Neurophysiol.* **105** (6), 2675–2686 (2011).

89. Bender, F. et al. Theta oscillations regulate the speed of locomotion via a hippocampus to lateral septum pathway. *Nat. Commun.* **6**, 8521 (2015).

90. Villette, V. et al. Decreased rhythmic GABAergic septal activity and memory-associated theta oscillations after hippocampal amyloid-beta pathology in the rat. *J. Neurosci.* **30** (33), 10991–11003 (2010).

91. Stoiljkovic, M. et al. Hippocampal network dynamics in response to alpha7 nACh receptors activation in amyloid-beta overproducing Transgenic mice. *Neurobiol. Aging.* **45**, 161–168 (2016).

92. Sargolini, F. et al. Conjunctive representation of position, direction, and velocity in entorhinal cortex. *Science* **312** (5774), 758–762 (2006).
93. Wills, T. J., Barry, C. & Cacucci, F. The abrupt development of adult-like grid cell firing in the medial entorhinal cortex. *Front. Neural Circuits.* **6**, 21 (2012).
94. Hinman, J. R. et al. Multiple running speed signals in medial entorhinal cortex. *Neuron* **91** (3), 666–679 (2016).
95. Nitz, D. & McNaughton, B. Differential modulation of CA1 and dentate gyrus interneurons during exploration of novel environments. *J. Neurophysiol.* **91** (2), 863–872 (2004).
96. Maurer, A. P. et al. Self-motion and the origin of differential Spatial scaling along the septo-temporal axis of the hippocampus. *Hippocampus* **15** (7), 841–852 (2005).
97. Klausberger, T. et al. Brain-state- and cell-type-specific firing of hippocampal interneurons in vivo. *Nature* **421** (6925), 844–848 (2003).
98. Forro, T. et al. Temporal organization of GABAergic interneurons in the intermediate CA1 hippocampus during network oscillations. *Cereb. Cortex.* **25** (5), 1228–1240 (2015).
99. Dannenberg, H. et al. The firing rate speed code of entorhinal speed cells differs across behaviorally relevant time scales and does not depend on medial septum inputs. *J. Neurosci.* **39** (18), 3434–3453 (2019).
100. Crown, L. M. et al. Aged rats exhibit altered Behavior-Induced oscillatory activity, place cell firing rates, and spatial information content in the CA1 region of the hippocampus. *J. Neurosci.* **42** (22), 4505–4516 (2022).
101. Gois, Z. & Tort, A. B. L. Characterizing speed cells in the rat hippocampus. *Cell. Rep.* **25** (7), 1872–1884 (2018). e4.

Author contributions
HN and ZZG wrote the manuscript and designed the study; JW designed the study; and ZLZ analyzed the data; CYX and MX performed the study; GHZ and DHW performed critical comments on the whole process of this study.

Declarations

Competing interests
The authors declare no competing interests.

Ethics approval and consent to participate
Our study is reported in accordance with ARRIVE guidelines. All experimental procedures involving animals were conducted according to the "Principles of laboratory animal care" (NIH publication No. 86 – 23, revised 1985), and were approved by the Animals Research Ethics Committee of Shanghai University of Chinese Medicine (No. PZSHUTCM2212260003).

Consent for publication
All authors agree to the publication of this manuscript.

Additional information
Supplementary Information The online version contains supplementary material available at https://doi.org/10.1038/s41598-025-95585-8.

Correspondence and requests for materials should be addressed to G.Z. or D.W.

Reprints and permissions information is available at www.nature.com/reprints.

Publisher's note Springer Nature remains neutral with regard to jurisdictional claims in published maps and institutional affiliations.